Virologica Sinica 37 (2022) 380–389

Contents lists available at ScienceDirect

Virologica Sinica

journal homepage: www.keaipublishing.com/en/journals/virologica-sinica
www.virosin.org

Research Article

Cytoplasmic domain and enzymatic activity of ACE2 are not required for PI4KB dependent endocytosis entry of SARS-CoV-2 into host cells

Hang Yang [a], Huijun Yuan [a], Xiaohui Zhao [a], Meng Xun [a], Shangrui Guo [a], Nan Wang [b], Bing Liu [c,d], Hongliang Wang [a,e,*]

[a] Department of Pathogen Biology and Immunology, School of Basic Medical Sciences, Xi'an Jiaotong University Health Science Center, Xi'an, 710061, China
[b] School of Pharmacy, Xi'an Jiaotong University Health Science Center, Xi'an, 710061, China
[c] BioBank, The First Affiliated Hospital of Xi'an Jiaotong University, Xi'an, 710061, China
[d] Department of Life Sciences, Faculty of Natural Sciences, Imperial College London, London, SW7 2AZ, United Kingdom
[e] Key Laboratory of Environment and Genes Related to Diseases, Xi'an Jiaotong University, Xi'an, 710061, China

ARTICLE INFO

Keywords:
SARS-CoV-2
Endocytosis
Phosphoinositides
Angiotensin converting enzyme 2 (ACE2)
Syncytium

ABSTRACT

The recent COVID-19 pandemic poses a global health emergency. Cellular entry of the causative agent SARS-CoV-2 is mediated by its spike protein interacting with cellular receptor-human angiotensin converting enzyme 2 (ACE2). Here, by using lentivirus based pseudotypes bearing spike protein, we demonstrated that entry of SARS-CoV-2 into host cells was dependent on clathrin-mediated endocytosis, and phosphoinositides played essential roles during this process. In addition, we showed that the intracellular domain and the catalytic activity of ACE2 were not required for efficient virus entry. Finally, we showed that the current predominant Delta variant, although with high infectivity and high syncytium formation, also entered cells through clathrin-mediated endocytosis. These results provide new insights into SARS-CoV-2 cellular entry and present proof of principle that targeting viral entry could be an effective way to treat different variant infections.

1. Introduction

Since the beginning of this century, there have been three beta-coronaviruses crossed the species barrier to cause severe respiratory diseases. In 2002–2003, severe acute respiratory syndrome coronavirus (SARS-CoV) infected 8096 people and caused 774 deaths (de Wit et al., 2016). In 2012, Middle East respiratory syndrome coronavirus (MERS-CoV) was discovered as the causative agent of a severe respiratory syndrome in the Middle East area and as of January 2020, more than 2500 people were diagnosed with MERS, with 866 associated deaths (Alotaibi and Bahammam, 2021). In late 2019, a novel coronavirus, named SARS-CoV-2 emerged and soon transmitted to cause a global pandemic. All three coronaviruses are believed to originate from bats but zoonotic transmission might involve different intermediate hosts. With numerous coronaviruses in bats, it is likely that coronavirus crises will continue to occur in the foreseeable future (Hu et al., 2015). Due to accumulated mutations and selection pressures during circulating, SARS-CoV-2 has evolved to different variants, among which, Alpha (B.1.1.7), Beta (B.1.351), Gamma (P.1) and Delta (B.1.617.2) have been listed as variants of concern (VOCs) by the WHO (WHO, 2021). Delta variant is currently the predominant variant of virus worldwide and it is more infectious with increased transmissibility compared to other variants and has been reported to have reduced sensitivity to antibody neutralization (Mlcochova et al., 2021; Planas et al., 2021).

Cellular entry of coronavirus is mediated by its spike glycoprotein (S) interacting with cellular receptors. The sequences of SARS-CoV and SARS-CoV-2 S protein are conserved and numerous studies have shown that they both exploit the same receptor, angiotensin-converting enzyme 2 (ACE2) (Hoffmann et al., 2020; Ou et al., 2020; Walls et al., 2020; Wrapp et al., 2020). Different from SARS-CoV, however, the S protein of SARS-CoV-2 was efficiently processed into two subunits, S1 and S2, which mediates attachment and membrane fusion, respectively (Hoffmann et al., 2020; Walls et al., 2020). Structural analysis showed that S protein formed trimer with the receptor-binding domain exposed up for easy receptor accessibility (Walls et al., 2020; Wrapp et al., 2020). ACE2 is a type I transmembrane protein with an extracellular domain with homology to ACE and a short cytoplasmic tail (Hamming et al., 2007; Lambert, 2009). It is a zinc metalloprotease that catalyzes the cleavage of Ang I to Ang1–9, but this catalytic activity has been shown not to be

* Corresponding author.
E-mail address: hongliangwang@xjtu.edu.cn (H. Wang).

https://doi.org/10.1016/j.virs.2022.03.003
Received 10 November 2021; Accepted 4 March 2022
Available online 7 March 2022
1995-820X/© 2022 The Authors. Publishing services by Elsevier B.V. on behalf of KeAi Communications Co. Ltd. This is an open access article under the CC BY-NC-ND license (http://creativecommons.org/licenses/by-nc-nd/4.0/).

required for spike induced syncytia formation in SARS-CoV infection (Li et al., 2003).

The entry of enveloped viruses into cells is known to occur via two primary pathways, i.e. direct membrane fusion at the cell surface or endocytosis, and endocytosis is thought to be a pH-sensitive process (Barocchi et al., 2005). The endocytic pathways exploited by animal viruses to gain entry into host cells include clathrin-mediated endocytosis (CME), caveolae-dependent endocytosis, as well as poorly characterized routes such as clathrin- and caveolae-independent endocytosis (Kumari et al., 2010). Spike of SARS-CoV, MERS-CoV or SARS-CoV-2 can be triggered to fuse either at the plasma membrane or the endosomal membrane depending on protease availability (Tang et al., 2020; Koch et al., 2021). In addition, SARS-CoV has been shown to enter host cells via direct membrane fusion, CME or non-clathrin, non-caveolae-mediated endocytosis (Ng, 2003; Inoue et al., 2007; Wang et al., 2008), suggesting the virus might employ various strategies to expand its cellular tropism. Similarly, SARS-CoV-2 cellular entry has also been reported to depend on different proteases (Hoffmann et al., 2020; Ou et al., 2020).

Phosphoinositides (PI) are known to be involved in the whole process of endocytosis (Kaksonen and Roux, 2018), and of note, PI(4,5)P_2 has been thought to be the most important PI during CME (Itoh and Takenawa, 2004; Haucke, 2005; Zoncu et al., 2007; McMahon and Boucrot, 2011; Posor et al., 2015). A recent study demonstrated that a successive PI molecular conversions accompanies the clathrin-coated pit assembly, budding and uncoating with PI(4,5)P_2, PI4P, PI(3,4)P_2 function at different stages of CME (He et al., 2017). Interestingly, SARS-CoV has been reported to require phosphatidylinositol 4-kinase beta (PI4KB) for cell entry and depletion of PI4P by phosphoinositide phosphatase Sac1 inhibited viral entry (Yang et al., 2012), suggesting a role of PI4P during viral entry. In contrast, inhibitors targeting PI(3,5)P_2 blocked SARS-CoV-2 viral entry (Ou et al., 2020). Whether other PI molecules are required for SARS-CoV-2 entry is still unknown.

Here we demonstrated that SARS-CoV-2 as well as the Delta variant entered cells via CME, but independent of caveolae-mediated endocytosis. Distinct from SARS-CoV, SARS-CoV-2 did not seem to require lipid rafts for infection of Huh7 cells. In addition, phosphatidylinositol molecules PI4P and PI(4,5)P_2 also played essential roles during virus entry. Finally, we showed that the cytoplasmic domain and the enzymatic activity of ACE2 were not required for SARS-CoV-2 entry. Our data provide new insights into SARS-CoV-2 cellular entry and present potential targets for drug development.

2. Materials and methods

2.1. Cell lines and constructs

Huh 7, Vero E6 and 293T cells were grown in Dulbecco's modified Eagle medium (DMEM) supplemented with 10% fetal bovine serum (FBS), nonessential amino acids, 100 U/mL of penicillin, and 100 μg/mL of streptomycin.

ACE2, Sac1 and inositol polyphosphate-5-phosphatase E (INPP5E) were amplified from cDNA library prepared with Huh 7 cells and each was cloned into a lentiviral expression vector pSMPUW. ACE2 truncation and mutants were obtained with overlap extension PCR amplification. Codon-optimized spike of SARS-CoV-2 (accession number: QLH58144.1) was purchased from GenScript (Cat#: MC_0101081) and subcloned to pcDNA3.1. $Spike_{fur/mut}$ (Q_{677}TILRSV_{683}) was obtained with overlap extension PCR amplification and $Spike_{delta}$ (L452R, T478K, and P681R) was obtained with Gibson Assembly (NEBuilder HiFi DNA Assembly). All primers used were listed in Supplementary Table S1. All constructs were confirmed by sequencing.

293T-ACE2 stable cell lines were generated by transfecting 293T cells with pSMPUM-ACE2 and selected with blasticidin. Antibiotic-resistant single clones were screened with immunoblotting and high ACE2-expressing clones were expanded for future use.

2.2. Antibodies and reagents

Antibodies used in this study include: SARS-CoV-2 spike (#GTX632604, GeneTex, Taiwan, China), HA tag (#3724, Cell Signaling Technology, Danvers, MA), early endosomal antigen 1 (EEA1, #3288, Cell Signaling Technology, Danvers, MA), HIV-p24 (#11695-R002, SinoBiological, Beijing, China), β-actin (#AC006, ABclonal, Woburn, MA), TMPRSS2 (sc-515727) and clathrin heavy chain (CHC, sc-12734) (Santa Cruz Biotechnology, Dallas, TX), caveolin-1 (CAV1, #16447-1-AP, Proteintech, Chicago, IL) and ACE2 (#CY5787, Abways Technology, Shanghai, China). PI4P (#Z-P004) and PI(4,5)P_2 (#Z-A045) antibodies were purchased from Echelon Biosciences.

DAPI (#D1306), Alexa Fluor conjugate cholera toxin subunit B (CTB, #C34775) and Alexa Fluor conjugated secondary antibodies for microscopy experiments were purchased from Life Technologies.

Chloroquine (#C6628), ammonium chloride (#254134), bafilomycin A1 (#19–148), chlorpromazine (CPZ, #C8138), filipin III (#F4767), methyl-β-cyclodextrin (MβCD, #C4555) were purchased from Sigma. Pitstop (#ab120685) was purchased from Abcam. PIK93 (#HY-12046), Wortmannin (#HY-10197), camostat mesylate (#HY-13512) and E−64d (#HY-100229) were purchased from MedChemExpress.

2.3. Pseudovirus preparation and titration

Pseudovirus was prepared with a previously described protocol (Ou et al., 2020) with minor modification. Briefly, 293T cells were co-transfected with lentiviral packaging plasmid psPAX2, pSMPUW engineered with either GFP or NanoLuc luciferase and glycoprotein expressing plasmid (pcDNA3.1-Spike, pMD2.G, or empty vector). At 48 h, 68 h post-transfection, virus supernatants were harvested and filtered through 0.45 μm pore-size filters. Viral supernatants were then used directly or concentrated through centrifuging at 100,000×*g* for 2 h in Himac ultracentrifuge S52ST rotor at 4 °C over a 20% sucrose solution, and virus stocks were resuspended with PBS and frozen at −80 °C. To titrate virus, RNAs from virus supernatant or concentrated virus stock were first extracted with viral RNA extraction kit (Tiangen, China) and reverse transcribed with RevertAid Reverse Transcription kit (Thermo Fisher Scientific). cDNAs from viral stock as well as series dilution of psPAX2 construct were quantitated with qPCR with primers targeting the gag encoding region (Supplementary Fig. S1C). A standard curve was generated with psPAX2 serial dilutions (Supplementary Fig. S1D) and the amount of virus in viral stock was interpolated and expressed as genome equivalents/mL (GEqs/mL). The primers used are listed in Supplementary Table S2.

2.4. Pseudovirus entry and inhibition study

Unless otherwise indicated, Huh 7 cells were used for entry assays. To transduce cells with pseudovirus, cells seeded in 24-well plate were inoculated with 30 μL of concentrated pseudovirus. About 36 h post-inoculation, cells were lysed and NanoLuc luciferase activity was measured with Nano-Glo® Luciferase Assay System (Promega, Madison, WI) according to manufacturer's instructions using a Synergy Neo 2 plate reader (BioTek, Winooski, VT). For phosphatase inhibition test, 293T-ACE2 cells were first transfected with Sac1 or INPP5E. And 30 h later, cells were split for immunoblotting and pseudovirus transduction. For ACE2 mutant assay, 293T cells were transfected with ACE2 or the indicated ACE2 mutant and 30 h later, cells were split for immunoblotting and pseudovirus transduction. For cells transduced with GFP pseudovirus, photos were taken at 56 h post-inoculation. For virus entry inhibition studies, cells were pretreated with indicated concentrations of inhibitors

for 1 h at 37 °C before pseudovirus inoculation. NanoLuc luciferase activity was measured as described above.

2.5. Immunoblotting and qPCR

Immunoblotting and qPCR were carried out as previously reported (Yang et al., 2021). Briefly, for immunoblotting, cells were lysed with LDS sample buffer (Thermo Fisher Scientific) and subjected to SDS-PAGE followed by transferring to a PVDF membrane. The blots were then probed with indicated antibodies and bands were visualized with SuperSignal™ West Femto Maximum Sensitivity Substrate (Thermo Fisher Scientific). For S protein incorporation test, pseudoviruses were first ultracentrifuged as described above and then subjected to SDS-PAGE. To quantify phosphatidylinositol 4-kinase β (PI4KB) mRNA, total RNAs from control or shRNA transduced cells were extracted with GeneJET RNA Purification Kit and then reversed transcribed with random primer and RevertAid Reverse Transcription kit (Thermo Fisher Scientific). Quantification was performed by real-time quantitative PCR with SYBR Mix (Genstar qPCR Master Mix) using specific primers listed in Supplementary Table S2.

2.6. Immunofluorescence staining

Immunofluorescence staining (except for ACE2 staining) was performed as described in (Yang et al., 2021). Images were taken with a Nikon C2 laser scanning confocal microscope in sequential scanning mode to limit crosstalk between fluorochromes. Quantitative colocalization was analyzed by NIH Image J with JACoP plugin (Bolte and Cordelieres, 2006). To stain ACE2 and mutants expression on cell surface, cells were fixed without any detergent treatment to keep cell membrane intact. Cells were then stained with anti-ACE2 antibody followed by Alexa-488 goat anti-rabbit secondary antibody.

2.7. shRNA knockdown or CRISPR knockout cell lines construction

VSV-G pseudotyped shRNA or CRISPR lentiviruses were produced as previously reported (Yang et al., 2021). Briefly, 293T cells were co-transfected with psPAX2, pMD2.G and pLKO.1-Puro based shRNA or pLentiCRISPR V2 based sgRNA lentiviral vectors and supernatants were harvested and used for transduction. sgRNA sequences and shRNA sequences used were listed in Supplementary Table S3. Cells transduced with lentiviral particles were then selected with puromycin for stable cell lines.

2.8. Statistical analysis

All values represent means ± standard deviations and represent the results of a minimum of three independent experiments. Where applicable, the two-tailed Student's *t*-test was used to compare the means of control and experimental groups.

3. Results

3.1. Incorporation of S protein into pseudovirus and infection of pseudovirus on different cells

Pseudovirus has been widely used to mimic the entry of real virus and is a powerful tool for studying early events in the life cycle of a virus. We here employed a lentivirus-based pseudovirus to study the entry of SARS-CoV-2. A codon-optimized cDNA encoding the S protein was employed, and the C-terminal last 19 amino acids, which contain an endoplasmic reticulum retention signal were replaced with FLAG tag (Supplementary Fig. S1A). We first showed that codon-optimization enhanced S protein expression in 293T cells (Supplementary Fig. S1B). In addition, consistent with previous reports (Hoffmann et al., 2020; Ou et al., 2020; Walls et al., 2020), the S protein was processed and two major bands were observed, reflecting the full-length and cleaved S proteins respectively (Supplementary Fig. S1B). To confirm S protein was efficiently incorporated into the pseudoviral particles, S protein-bearing pseudoviruses (S pseudoviruses) were pelleted by ultracentrifugation and tested against anti-spike antibody (Fig. 1A). The results showed that S protein was incorporated into viral particles and the majority of S proteins on pseudovirus were also cleaved, further suggesting the S protein was efficiently processed in host cells.

Next, we tested whether these S pseudoviruses were able to transduce host cells. For this purpose, we infected 293T, Vero E6, Huh 7 and 293T cells overexpressing ACE2 (293T-ACE2) with S or VSV-G protein pseudovirus containing a luciferase reporter gene. While VSV-G pseudovirus could transduce all four cell types efficiently, S pseudovirus showed different transduction on these cells (Fig. 1B). First, 293T cells could be transduced by S pseudoviruses, although at low level compared to other cells. On the other hand, overexpression of ACE2 in 293T cells significantly enhanced S pseudovirus infection. Immunoblotting showed that there was low level of ACE2 expression in 293T cells, while 293T-ACE2 had significantly enhanced ACE2 expression (Fig. 1C). These results revealed a correlation between ACE2 expression and S pseudovirus transduction, suggesting SARS-CoV-2 utilizes ACE2 as a receptor. Although both Vero E6 and Huh 7 cells had moderate ACE2 expression and could be transduced by S pseudovirus efficiently, Huh 7 gave more than two-fold luciferase activity than Vero E6 cells (Fig. 1B and C). Similarly, GFP-expressing pseudoviruses also transduced the above cells lines successfully and Huh 7 cells showed more positive cells than Vero E6 cells (Fig. 1D). Therefore, Huh 7 was chosen for the following viral entry studies.

3.2. S pseudovirus enters cells via CME

The entry of SARS-CoV-2 into host cells requires the activation of its surface spike protein by cell surface serine protease TMPRSS2 or endosomal cysteine proteases cathepsin B/L (Hoffmann et al., 2020). We next tested whether SARS-CoV-2 entry into Huh 7 cells could be blocked by TMPRSS2 inhibitor, camostat mesylate or cathepsin inhibitor, E-64d. Fig. 2A showed that camostat mesylate did not interfere with SARS-CoV-2 entry into Huh 7 cells, which was blocked by E-64d in a dose-dependent manner. Cellular ATP content measurement showed that neither drug caused cytotoxicity (Supplementary Fig. S2A). Consistent with this, we found that Huh 7 cells had relatively low TMPRSS2 expression compared to Caco2 cells (Supplementary Fig. S2B), which has been shown to be sensitive to camostat mesylate (Hoffmann et al., 2020). These results suggested that SARS-CoV-2 could use endosomal proteases for spike priming during Huh 7 cell infection. We then tested whether SARS-CoV-2 could enter cells via endocytosis. In contrast to direct membrane fusion, endocytosis is thought to be pH-dependent (White and Whittaker, 2016). When Huh 7 cells were pretreated with lysosomotropic agents, like chloroquine, ammonium chloride or bafilomycin A1, significant decrease of transduction was observed for both VSV-G and SARS-CoV-2 S pseudoviruses without causing any cytotoxicity (Fig. 2B, Supplementary Fig. S2C), suggesting that SARS-CoV-2 entry of Huh 7 cells was pH-dependent. Dual immunostaining of S protein and early endosome marker EEA1 showed colocalization [Fig. 2C, Pearson correlation coefficient (Pr) = 0.583], further supporting that S pseudovirus infected Huh 7 cells via endocytosis.

CME is the best documented mode of endocytosis. Pretreatment of Huh 7 cells with clathrin inhibitor, pitstop (von Kleist et al., 2011) inhibited the entry of SARS-CoV-2 or VSV-G pseudovirus in a dose-dependent manner (Fig. 2D). Similarly, CPZ, which prevents the assembly of coated pits at the cell surface, also inhibited the entry of SARS-CoV-2 or VSV-G pseudovirus in a dose-dependent manner (Fig. 2E). Both drugs showed little cytotoxicity with the concentrations tested (Supplementary Figs. S2D and E). These results suggest CME is involved during SARS-CoV-2 infection of Huh 7 cells.

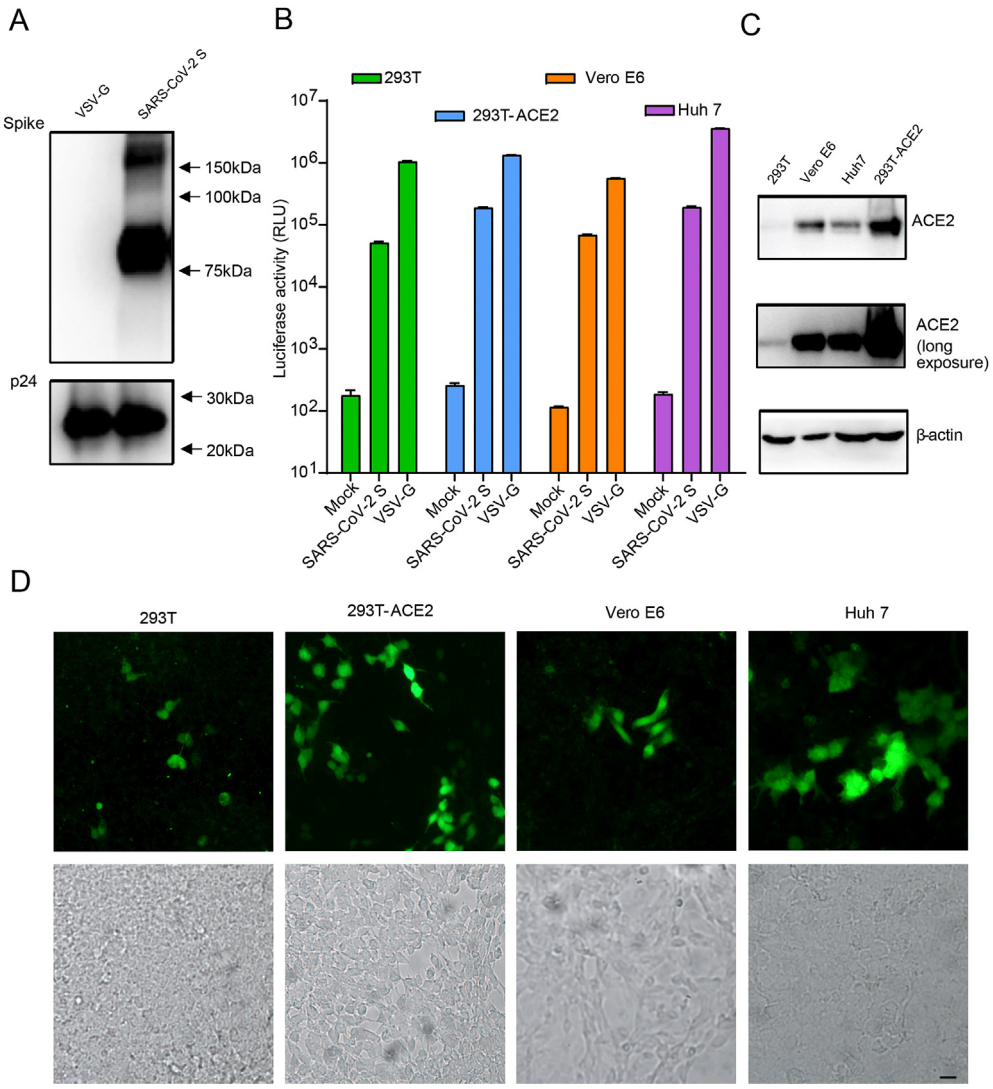

Fig. 1. Characterization of SARS-CoV-2 Spike pseudovirus. **A** Incorporation of SARS-CoV-2 S protein into pseudoviruses. VSV-G and S pseudoviruses were pelleted as described in materials and methods and subjected to SDS-PAGE, immunoblotted with anti-Spike and anti- HIV p24. **B** S pseudovirus transduction of 293T, 293T-ACE2, Vero E6 and Huh 7 cells. 293T, 293T-ACE2, Vero E6 and Huh 7 cells were infected with equal amounts of (5×10^7 GEqs) pseudovirus without glycoprotein (mock), S pseudovirus, or VSV-G pseudovirus expressing NanoLuc luciferase. At 48 h post-transduction, luciferase activity was measured. Values were mean ± SD and are representative of three independent experiments. **C** ACE2 expression in 293T, Vero E6, Huh 7 and 293T-ACE2 cells. 293T, Vero E6, Huh 7 and 293T-ACE2 cell lysates were immunoblotted with anti-ACE2 and anti-β-actin antibodies. **D** 293T, 293T-ACE2, Vero E6 and Huh 7 cells transduced with S pseudovirus expressing GFP. Bright field was included to show the presence of cells. Scalebar, 20 μm. S, spike; SD, standard deviation; GEqs, genome equivalents.

To overcome any nonspecific effect the chemical compounds may have, we also carried out an orthogonal CRISPR/Cas9 knockout experiment. Huh 7 cells stably transduced with lentiviral vectors encoding the sgRNA targeting CHC and *Streptococcus pyogenes* Cas9 were first validated of gene targeting (Fig. 2F inset) and then transduced with S pseudovirus encoding luciferase. The magnitude of luciferase activity correlated with the expression of CHC (Fig. 2F), strongly suggesting that SARS-CoV-2 entry was dependent on clathrin.

3.3. S pseudovirus infection does not require caveolae-mediated endocytosis

Caveolae are small, flask-shaped invaginations in the plasma membrane composed of high levels of cholesterol and glycosphingolipids as well as the integral membrane protein caveolin (Stan, 2005). CTB has been reported to be internalized via caveolae-mediated endocytosis (Montesano et al., 1982; Tran et al., 1987; Orlandi and Fishman, 1998) and treatment of cells with filipin or methyl-β-cyclodextrin (MβCD) would disrupt the integrity of cholesterol-enriched membrane microdomains (Lu et al., 2016). We found that filipin or MβCD treatment did not cause any cytotoxicity (Supplementary Figs. S3A and B), but pretreatment of Huh 7 cells with either drug blocked the uptake of CTB (Supplementary Fig. S3C), suggesting the concentrations we used could block caveolae-mediated endocytosis. However, neither drug inhibited the S pseudovirus or VSV-G pseudovirus transduction (Fig. 3A and B), indicating that SARS-CoV-2 entry of Huh 7 cells was independent of cholesterol-enriched membrane microdomains.

To further elucidate the role of caveolae-dependent pathway in SARS-CoV-2 infection, we inhibited the expression of CAV1 (Fig. 3C) with CRISPR/Cas9. Fig. 3D showed that S pseudovirus could infect Huh 7 cells in the absence of CAV1, suggesting the viral entry was independent of caveolae. This finding was further corroborated by the immunostaining experiment, which showed little colocalization between SARS-CoV-2 spike protein and CAV1 (Fig. 3E, Pr = 0.064). Taken together, these results indicate that SARS-CoV-2 entry is independent of caveolae-mediated endocytosis.

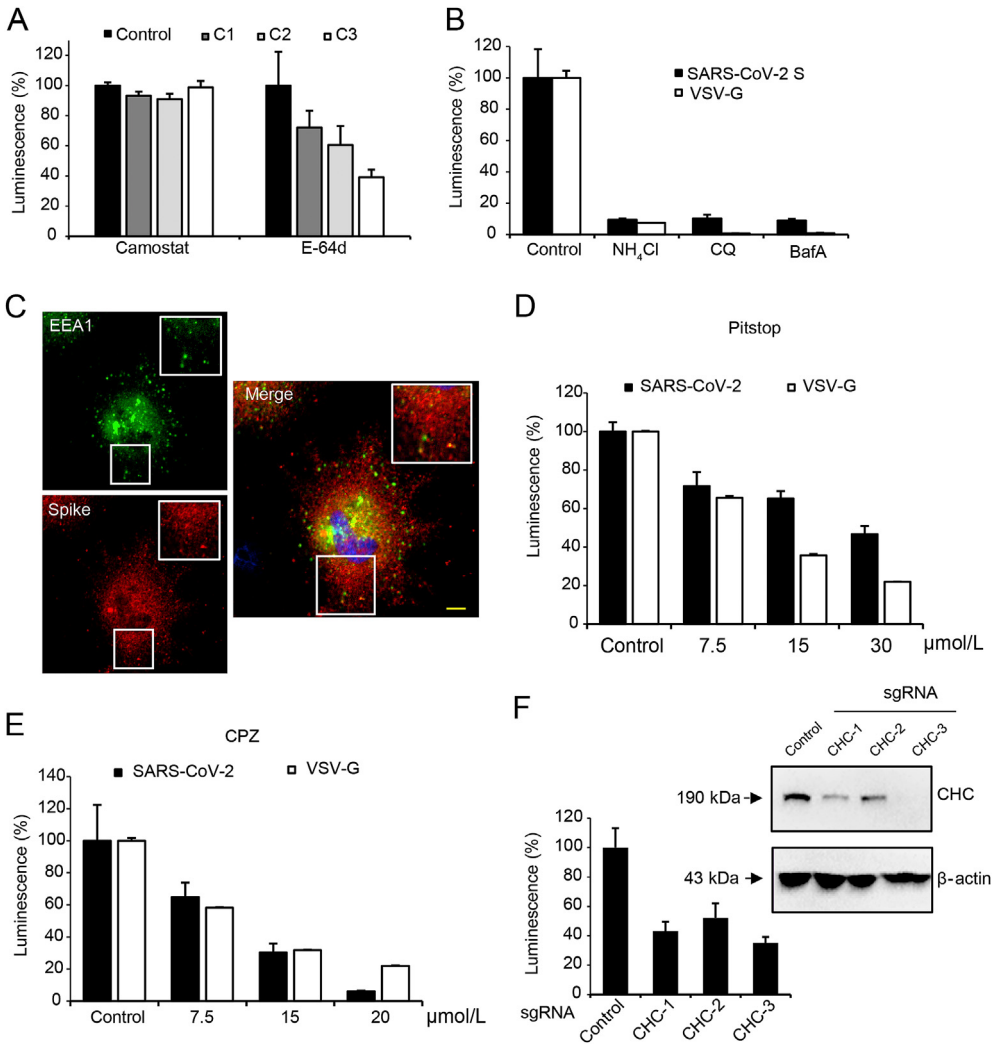

Fig. 2. S pseudovirus transduces Huh 7 cells via clathrin-mediated endocytosis. **A** Huh 7 cells pretreated with different concentrations of camostat mesylate (5, 15, 50 μmol/L) or E-64d (5, 10, 25 μmol/L) were transduced with S pseudovirus and luciferase was measured. Values were normalized to control and expressed as mean ± SD. **B** Huh 7 cells pretreated with lysosomotropic agents (50 mmol/L NH_4Cl, 100 μmol/L chloroquine and 100 nmol/L bafilomycin A) were transduced with S pseudovirus or VSV-G pseudovirus. Luciferase was measured to indicate viral infection. Values were normalized to control and expressed as mean ± SD. **C** Immunostaining of S pseudovirus infected Huh 7 cells for Spike (red) and EEA1 (green). Scalebar, 10 μm. **D** Huh 7 cells pretreated with indicated concentrations of pitstop were transduced with S pseudovirus or VSV-G pseudovirus and luciferase was measured. Values were normalized to control and expressed as mean ± SD. **E** Huh 7 cells pretreated with indicated concentrations of CPZ were transduced with S pseudovirus or VSV-G pseudovirus and luciferase was measured. Values were normalized to control and expressed as mean ± SD. **F** Huh 7 cells stably expressing a negative control or three independent CHC sgRNAs with Cas9 were transduced with S pseudovirus and luciferase was measured. Values were normalized to control and expressed as mean ± SD. Inset, immunoblotting of CHC expression in Huh 7 cells as described above. S, spike; CQ, chloroquine; Baf A, bafilomycin A; CPZ, chlorpromazine; CHC, clathrin heavy chain; SD, standard deviation.

3.4. *PI4P and PI(4,5)P_2 are crucial for SARS-CoV-2 entry*

PI is known to be involved throughout the process of endocytosis. Of note, PI(4,5)P_2, PI4P and PI(3,4)P_2 are essential molecules in endocytosis. We found that overexpression of either INPP5E, which converted PI(4,5)P_2 to PI4P, or the sac1 phosphatase, which dephosphorylated PI4P (Fig. 4A, Supplementary Fig. S4A), inhibited S pseudovirus transduction without cytotoxicity (Fig. 4B, Supplementary Fig. S4B), suggesting that PI4P and PI(4,5)P_2 were involved in SARS-CoV-2 entry. Importantly, pretreatment of Huh 7 cells with phosphatidylinositol kinase inhibitors, PIK93 or wortmannin, inhibited S pseudovirus transduction at concentrations that effectively inhibited PI4-kinase activity (Fig. 4C, Supplementary Figs. S4D and E), suggesting that PI4 kinase was involved in SARS-CoV-2 infection. As PI4KB has been shown to be involved in SARS-CoV infection (Yang et al., 2012), we next tested whether it is also required for SARS-CoV-2 infection. For this purpose, we first knocked down PI4KB expression with shRNAs, and qPCR results showed that all three shRNAs could efficient target PI4KB expression (Fig. 4D open bars, Supplementary Fig. S4C). When these cells were infected with S pseudovirus, we found that PI4KB knockdown led to significant decrease in SARS-CoV-2 transduction (Fig. 4D, black bars), suggesting PI4KB was required for SARS-CoV-2 infection.

3.5. *SARS-CoV-2 entry does not require the intracellular domain and catalytic sites of ACE2*

Receptor-mediated endocytosis involves the interaction of the cytoplasmic tails of the receptor proteins with intracellular proteins to initiate internalization (Marks et al., 1997; McPherson et al., 2001; Sorkin and von Zastrow, 2009), and studies have shown that cytoplasmic domain of cell surface receptors can control endocytosis (Miettinen et al., 1992; Morse et al., 2014). ACE2 is a type I transmembrane protein with a short

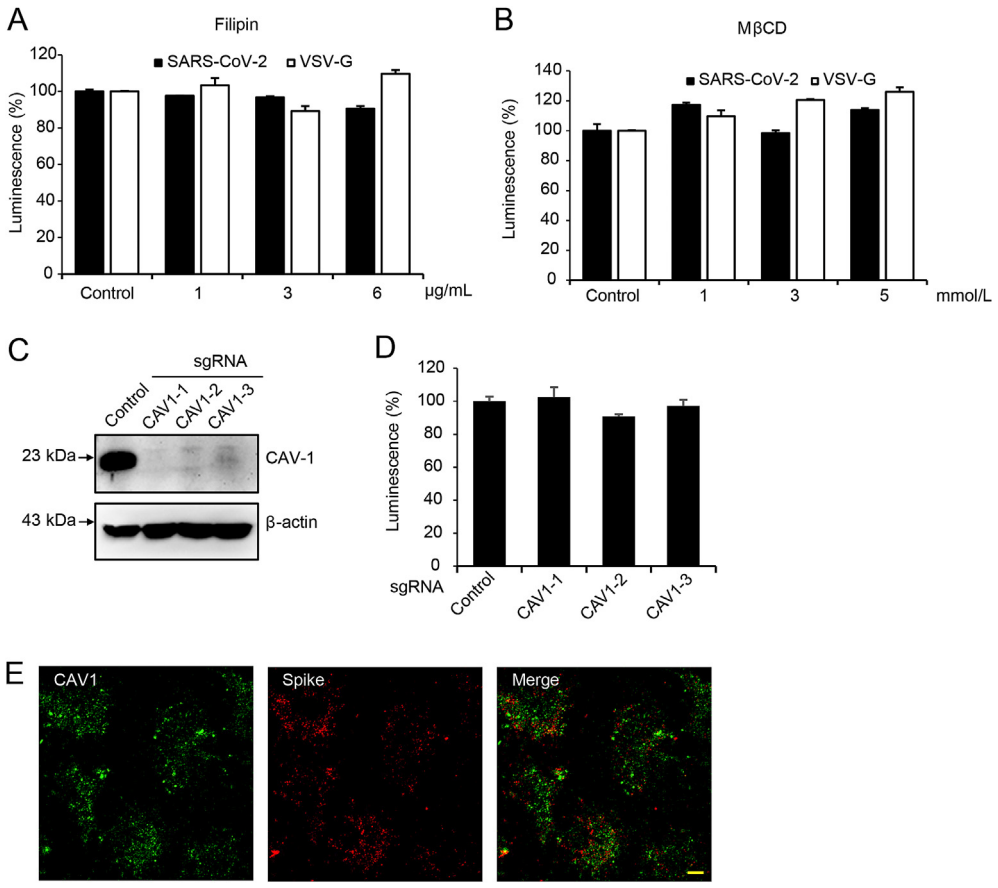

Fig. 3. S pseudovirus transduces Huh 7 cells independent of caveolae-mediated endocytosis. **A**–**B** Huh 7 cells pretreated with indicated concentrations of filipin (**A**) or MβCD (**B**) were transduced with S pseudovirus or VSV-G pseudovirus and luciferase was measured. Values were normalized to control and expressed as mean ± SD. **C** Immunoblotting of CAV1 expression in Huh 7 cells stably expressing a negative control or three independent CAV1 sgRNAs with Cas9. **D** Huh 7 cells as treated in (**C**) were transduced with S pseudovirus and luciferase was measured. Values were normalized to control and expressed as mean ± SD. **E** Immunostaining of S pseudovirus infected Huh 7 cells for Spike (red) and CAV1 (green). Scalebar, 10 μm. CAV1, caveolin-1; MβCD, methyl-β-cyclodextrin; S, spike; SD, standard deviation.

cytoplasmic tail (Hamming et al., 2007; Lambert, 2009). We therefore tested whether the cytoplasmic tail of ACE2 was required for SARS-CoV-2 entry. For this experiment, 293T cells with low transduction rate was chosen as reference and cells expressing either wild-type ACE2 or different mutant were then assayed for their ability to support S pseudovirus infection. We first showed that wild-type ACE2 or ACE2 mutants all expressed on cell surface (Supplementary Fig. S5), suggesting that these cells are proper models for S pseudovirus transduction. We then found that 293T cells overexpressing ACE2 mutant lacking the intracellular tail (ACE2-TM) could be infected by SARS-CoV-2 pseudovirus as efficiently as wild-type ACE2 (Fig. 5A–C). We then examined the receptor activity of ACE2 mutants with either the transmembrane domain of EGFR (ACE2-EGFR) or the transmembrane domain and cytoplasmic tail of human ACE (ACE2-ACE), the close homologue of ACE2 which could not support virus infection. Both mutants could support infection of SARS-CoV-2(Fig. 5A–C). These results together suggest that the cytoplasmic domain of ACE2 is not required for its SARS-CoV-2 infection and that there is no specificity of the transmembrane domain for its receptor activity.

We next tested whether the enzyme activity of ACE2 was required for SARS-CoV-2 infection. ACE2 is a zinc metalloprotease with a single HEXXH zinc-binding motif that is essential for its activity (Tipnis et al., 2000; Turner et al., 2002). In addition, ACE2 structure modeling and site-directed mutagenesis analysis showed that His_{505} played an essential role in the catalysis of ACE2 (Guy et al., 2003, 2005; Towler et al., 2004) (Fig. 5D). To test whether enzymatic activity of ACE2 was required for SARS-CoV-2 entry, 293T cells overexpressing ACE2 with two zinc-binding histidine mutations (H374 N&H378 N, CM1) were transduced with S pseudovirus. Fig. 5F showed that this mutant support viral infection equally well to wild type ACE2. Similarly, 293T cells overexpressing ACE2 catalytic site histidine mutation (H505L, CM2), or the combination of all three histidine mutations (H374 N&H378 N&H505L, CM3) could be transduced by S pseudovirus as efficiently (Fig.5D–F, Supplementary Fig. S5). These results suggest that the enzymatic activity of ACE2 is not required for SARS-CoV-2 infection.

3.6. *Delta variant enters cells via CME*

To study the cellular entry of Delta variant, we then made pseudoviruses bearing spike with the unique set of Delta mutations L452R, T478K, and P681R (Rahman et al., 2021) (Supplementary Fig. S6A). We found this $Spike_{delta}$ was present predominantly in the cleaved form compared to wild-type spike, while spike that has mutation in the furin cleavage site ($Spike_{fur/mut}$) mainly presented as uncleavaged form (Fig. 6A), suggesting the introduction of P681R mutation enhanced spike cleavage. Consistent with the fact that Delta variant has higher transmissibility, increased infectivity was also observed for $Spike_{delta}$ mediated cell entry (Fig. 6B). In addition, $Spike_{delta}$ also mediated higher cell fusion and syncytium formation than WT Spike, while the $Spike_{fur/mut}$ barely induced any syncytium formation (Fig. 6C and D), arguing the role of furin cleavage during virus infection and syncytium formation. However, $Spike_{delta}$ pseudovirus mediated entry could still be inhibited by CPZ or pitstop (Fig. 6E and F), suggesting this variant still enters cells via

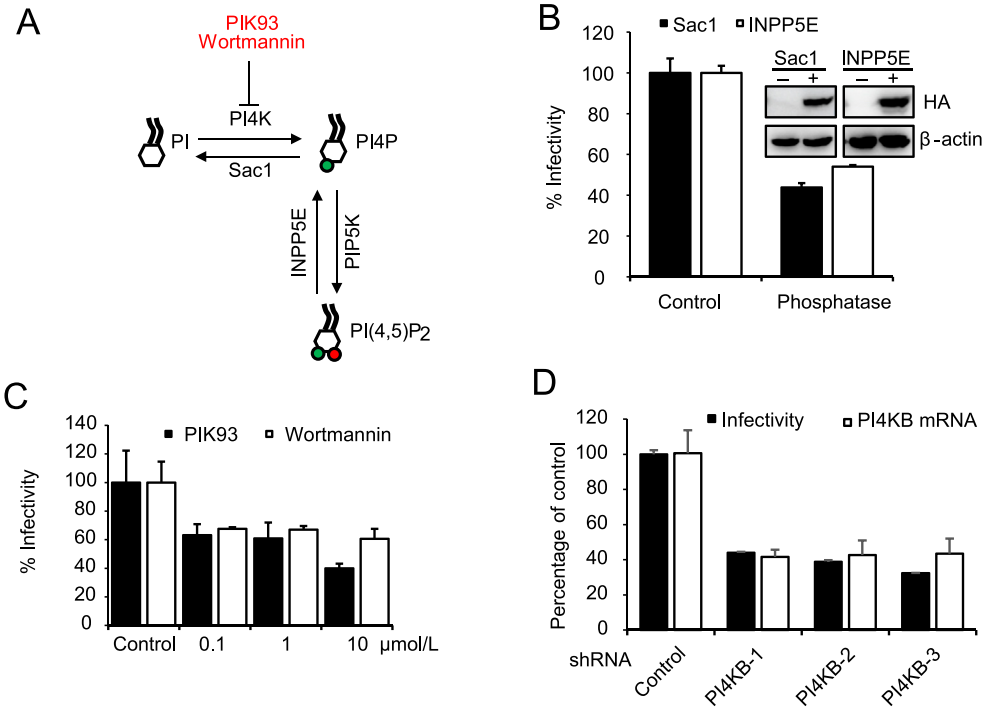

Fig. 4. PI4KB is relevant to S pseudovirus infection. **A** Diagram of phosphoinositide metabolic pathways. PIK93 and wortmannin were used as inhibitors targeting PI4K. **B** 293T-ACE2 cells were transfected with HA-Sac1 or HA-INPP5E before they were transduced with S pseudovirus and luciferase was measured. Values were normalized to control and expressed as mean ± SD. Inset, immunoblotting of HA-Sac1 or HA-INPP5E expression with anti-HA antibody. **C** Huh 7 cells pretreated with indicated concentrations of PIK93 or wortmannin were transduced with S pseudovirus and luciferase was measured. Values were normalized to control and expressed as mean ± SD. **D** Huh 7 cells transduced with the indicated shRNAs were infected with S pseudovirus and luciferase was measured to reflect viral infection (black bars). PI4KB mRNA was quantified by qRT-PCR (open bars). Values were normalized to control shRNA. PI4KB, phosphatidylinositol 4-kinase β; PI, Phosphoinositides; INPP5E, inositol polyphosphate-5-phosphatase E; PIP5K, Phosphatidylinositol-4-phosphate 5-kinase; S, spike; SD, standard deviation.

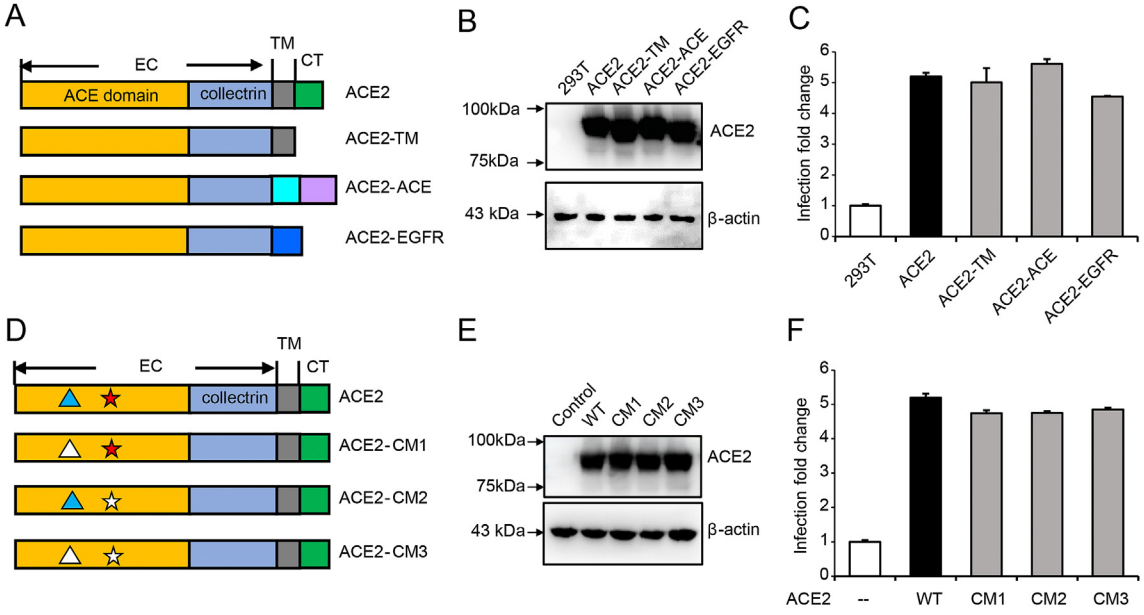

Fig. 5. Cytoplasmic domain and enzymatic activity of ACE2 are not required for S pseudovirus infection. **A** Diagram of ACE2 and ACE2 mutants. EC, extracellular domain. TM, transmembrane domain. CT, cytoplasmic tail. ACE2-TM, ACE2 lacking the cytoplasmic tail; ACE2-ACE, chimera of ACE2 with transmembrane and cytoplasmic tail form ACE; ACE2-EGFR, chimera of ACE2 with transmembrane domain form EGFR. **B** Immunoblotting of ACE2 and ACE2 mutants expression. **C** 293T cells transfected with wild type or indicated ACE2 mutant were transduced with S pseudovirus and luciferase was measured. Values were expressed as fold change to 293T cells. **D** Diagram of ACE2 and ACE2 catalytic dead mutants. "Δ" represents the zinc binding histidines and "★" indicates the catalytic active site histidine. Filled symbols represent wild type sequence and blank symbols represent mutations. **E** Immunoblotting of ACE2 and mutants expression. **F** 293T cells transfected with wild type or indicated ACE2 mutant were transduced with S pseudovirus and luciferase was measured. Values were expressed as fold change to 293T cells. CM, catalytic site mutation; S, spike; SD, standard deviation; WT, wild-type.

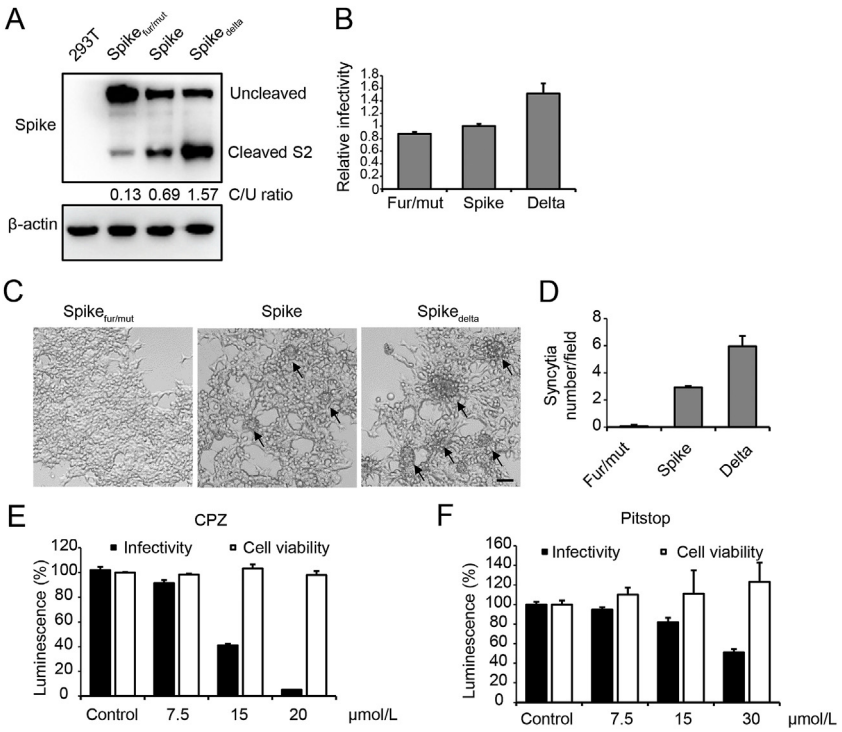

Fig. 6. Delta variant enters Huh 7 cells via clathrin-mediated endocytosis. **A** 293T cells were mock transfected or transfected with Spike, $Spike_{fur/mut}$, or $Spike_{delta}$ and subjected to immunoblotting with anti-Spike antibody. Cleaved and uncleaved spike were indicated. Band densities were quantified with Image J and the ratios of cleaved band density to that of uncleaved band were shown below. **B** Huh 7 cells transduced with 3×10^7 GEq pseudovirus bearing wild Spike, $Spike_{fur/mut}$, or $Spike_{delta}$ and luciferase was measured. Values from wild type spike were set to 1. **C** 293T-ACE2 cells were transfected with construct encoding Spike, $Spike_{fur/mut}$, or $Spike_{delta}$ and cell fusion were observed after 36 h. Arrows indicate syncytium formation. **D** Quantitation of numbers of syncytia in cells as described in (**C**). Values are syncytia number per microscope field. Scalebar, 100 μm. **E** Huh 7 cells pretreated with indicated concentrations of CPZ were transduced with pseudovirus bearing $Spike_{delta}$ and luciferase was measured. Values were normalized to control and expressed as mean ± SD. Cell viability was measured with Cell Titer Glo. **F** Huh 7 cells pretreated with indicated concentrations of pitstop were transduced with pseudovirus bearing $Spike_{delta}$ and luciferase was measured. Values were normalized to control and expressed as mean ± SD. Cell viability was measured with Cell Titer Glo. GEq, genome equivalents; S, spike; CPZ, chlorpromazine; SD, standard deviation.

CME. On the other hand, pretreatment of Huh 7 cells with either filipin or MβCD had little effect on $Spike_{delta}$ pseudovirus entry (Supplementary Fig. S6B), suggesting this variant, like its parental strain, does not depend on caveolae-mediated endocytosis.

4. Discussion

Viral entry represents the first step of virus-host interaction and glycoprotein-bearing pseudoviruses have been widely used for viral entry studies. Here we generated S pseudoviruses that had either a luciferase or GFP reporter gene. These viruses could transduce host cells expressing ACE2 receptor and therefore could be used for viral entry studies.

For enveloped viruses, the viral envelop must fuse with host membranes either at cell surface or in endosomes before the successful release of viral genome into host cells. SARS-CoV and MERS-CoV have been reported to utilize both pathways depending on the availability of exogenous and membrane bound proteases (Tang et al., 2020). The entry of SARS-CoV-2 has been reported to require cell surface protease TMPRSS2 (Hoffmann et al., 2020), suggesting direct membrane at cell surface was possible. In addition, several studies have demonstrated that lysosomotropic agents could block SARS-CoV-2 entry (Hoffmann et al., 2020; Ou et al., 2020), indicating the virus might also enter via endocytosis. Here we also found that lysosomotropic agents inhibited S pseudovirus transduction. In addition, we demonstrated colocalization of S protein with early endosome marker EEA1, further proving that this virus could enter cells via pH-dependent endocytosis.

As the best characterized endocytosis pathways, CME has been reported to be involved in various viral infection, including SARS-CoV (Inoue et al., 2007). Here by using different chemical inhibitors and CRISPR/Cas9 targeting the major protein in clathrin coat formation, we demonstrated that SARS-CoV-2 entry was also dependent on clathrin. While we are preparing this manuscript, Bayati et al. reported that the S protein of SARS-CoV-2 endocytosis was dependent on clathrin and S pseudovirus could be blocked by CHC siRNA treatment (Bayati et al., 2021). Consistently, we also showed that SARS-CoV-2 pseudovirus entered cells via CME. In addition, we showed that this process was independent of caveolae-mediated endocytosis, another common endocytosis pathway. The fact that Caco2 cells, which do not express caveolin (Mirre et al., 1996), could support SARS-CoV-2 infection efficiently (Chu et al., 2020) also suggested that this virus could infect cells independent of caveolae. Here we also showed filipin or MβCD treatment had little effect on SARS-CoV-2 entering Huh 7 cells, however, lipid rafts and cholesterol have been reported to be important for SARS-CoV-2 infection (Li et al., 2021a; Sanders et al., 2021). One explanation for this discrepancy is that SARS-CoV-2 may enter different cell types via different pathways. Just as virus may enter cells via plasma membrane fusion or endocytosis depending on whether TMPRSS2 is expressed (Koch et al., 2021), virus may also enter cells with or without cholesterol involvement. Consistent with this hypothesis, we found that SARS-CoV-2 entry of 293T-ACE2 cells was sensitive to MβCD pretreatment (Supplementary Fig. S6C), in agreement with a previous study (Li et al., 2021b). These results further suggest that viruses may exploit different molecules to gain infection of different cell types, expanding its cellular/tissue tropism.

As a virus with an RNA genome, coronaviruses have high mutation rates and the past months have witnessed the emergence of different SARS-CoV-2 variants. Among them, the Delta variant caused great concerns due to its high transmissibility and reduced vaccine efficacy

(Mlcochova et al., 2021; Planas et al., 2021). Here, by using pseudoviruses bearing Spike with Delta unique mutations, we showed that although this variant has high infectivity and causes increased syncytia formation, it still enters cells through CME. These results provided proof of principle that targeting viral entry could be an effective way to block different variants infections.

PI4P and PI4KB have been reported to be essential for SARS-CoV infection (Yang et al., 2012) and a recent report showed that PIKfyve inhibitors could block S pseudovirus infection (Ou et al., 2020), which all suggested that phosphoinositide pathways were important for coronavirus infection. Here we further demonstrated that PI4P and PI(4,5)P_2 were essential molecules for SARS-CoV-2 infection and PI4KB was also required for SARS-CoV-2 entry.

The role of cytoplasmic tail of ACE2 in SARS-CoV infection is controversial (Inoue et al., 2007; Haga et al., 2008), while Karthika et al. reported that SARS-CoV-2 cellular entry is independent of the ACE2 cytoplasmic domain (Karthika et al., 2021). We here showed that the cytoplasmic domain as well as the enzymatic activity of ACE2 were not required for efficient virus entry. These results were further supported by the Spike-ACE2 complex structure determined by X-ray crystallography or cryo-EM (Lan et al., 2020; Yan et al., 2020), which showed that the receptor-binding domain of S interacted with the N-terminal peptidase domain of ACE2 and the enzymatic sites were not in direct contacts with S protein.

5. Conclusions

In summary, here we found that the entry of SARS-CoV-2 into host cells was dependent on CME by using lentivirus based pseudotypes bearing spike proteins, and PI played essential roles during this process. Meanwhile, the intracellular domain and the catalytic activity of ACE2 are not required for efficient virus entry. In addition, Delta variant, which has high infectivity and high syncytium formation rate, also enters cells through CME. These results provide new insights into SARS-CoV-2 cellular entry and present proof of principle that targeting viral entry could be an effective way to treat different variant infections.

Data availability

All data generated or analyzed during this study are included in this published article.

Ethics statement

This article does not contain any studies with human or animal subjects performed by any of the authors.

Author contributions

Yang Hang: investigation, methodology, formal analysis. Yuan Huijun: methodology, validation. Zhao Xiaohui: methodology, validation. Xun Meng: validation, supervision. Wang Nan: validation, supervision. Guo Shangrui: investigation. Liu Bing: conceptualization, supervision. Wang Hongliang: conceptualization, methodology, funding acquisition, writing-reviewing and editing.

Conflict of interest

The authors declare that they have no conflict of interest.

Acknowledgements

This work was supported by the National Natural Science Foundation of China (81871662, 82150201), Xi'an Jiaotong University Fund (xzy012019066 and xzy032020037) and Xi'an Jiaotong University Health Science Center-Qinnong Bank Fund (QNXJTU-04& QNXJTU-07).

Appendix A. Supplementary data

Supplementary data to this article can be found online at https://doi.org/10.1016/j.virs.2022.03.003.

References

Alotaibi, M.H., Bahammam, S.A., 2021. Determining the correlation between comorbidities and mers-cov mortality in Saudi Arabia. J. Taibah. Univ. Med .Sci. 16, 591–595.
Barocchi, M.A., Masignani, V., Rappuoli, R., 2005. Opinion: cell entry machines: a common theme in nature? Nat. Rev. Microbiol. 3, 349–358.
Bayati, A., Kumar, R., Francis, V., McPherson, P.S., 2021. Sars-cov-2 infects cells following viral entry via clathrin-mediated endocytosis. J. Biol. Chem. 100306, 296.
Bolte, S., Cordelieres, F.P., 2006. A guided tour into subcellular colocalization analysis in light microscopy. J. Microsc. 224, 213–232.
Chu, H., Chan, J.F., Yuen, T.T., Shuai, H., Yuan, S., Wang, Y., Hu, B., Yip, C.C., Tsang, J.O., Huang, X., Chai, Y., Yang, D., Hou, Y., Chik, K.K., Zhang, X., Fung, A.Y., Tsoi, H.W., Cai, J.P., Chan, W.M., Ip, J.D., Chu, A.W., Zhou, J., Lung, D.C., Kok, K.H., To, K.K., Tsang, O.T., Chan, K.H., Yuen, K.Y., 2020. Comparative tropism, replication kinetics, and cell damage profiling of sars-cov-2 and sars-cov with implications for clinical manifestations, transmissibility, and laboratory studies of covid-19: an observational study. Lancet. Microbe. 1, e14–e23.
de Wit, E., van Doremalen, N., Falzarano, D., Munster, V.J., 2016. Sars and mers: recent insights into emerging coronaviruses. Nat. Rev. Microbiol. 14, 523–534.
Guy, J.L., Jackson, R.M., Acharya, K.R., Sturrock, E.D., Hooper, N.M., Turner, A.J., 2003. Angiotensin-converting enzyme-2 (ace2): comparative modeling of the active site, specificity requirements, and chloride dependence. Biochemistry 42, 13185–13192.
Guy, J.L., Jackson, R.M., Jensen, H.A., Hooper, N.M., Turner, A.J., 2005. Identification of critical active-site residues in angiotensin-converting enzyme-2 (ace2) by site-directed mutagenesis. FEBS J. 272, 3512–3520.
Haga, S., Yamamoto, N., Nakai-Murakami, C., Osawa, Y., Tokunaga, K., Sata, T., Yamamoto, N., Sasazuki, T., Ishizaka, Y., 2008. Modulation of tnf-alpha-converting enzyme by the spike protein of sars-cov and ace2 induces tnf-alpha production and facilitates viral entry. Proc. Natl. Acad. Sci. U. S. A. 105, 7809–7814.
Hamming, I., Cooper, M.E., Haagmans, B.L., Hooper, N.M., Korstanje, R., Osterhaus, A.D., Timens, W., Turner, A.J., Navis, G., van Goor, H., 2007. The emerging role of ace2 in physiology and disease. J. Pathol. 212, 1–11.
Haucke, V., 2005. Phosphoinositide regulation of clathrin-mediated endocytosis. Biochem. Soc. Trans. 33, 1285–1289.
He, K., Marsland III, R., Upadhyayula, S., Song, E., Dang, S., Capraro, B.R., Wang, W., Skillern, W., Gaudin, R., Ma, M., Kirchhausen, T., 2017. Dynamics of phosphoinositide conversion in clathrin-mediated endocytic traffic. Nature 552, 410–414.
Hoffmann, M., Kleine-Weber, H., Schroeder, S., Kruger, N., Herrler, T., Erichsen, S., Schiergens, T.S., Herrler, G., Wu, N.H., Nitsche, A., Muller, M.A., Drosten, C., Pohlmann, S., 2020. Sars-cov-2 cell entry depends on ace2 and tmprss2 and is blocked by a clinically proven protease inhibitor. Cell 181, 271–280 e278.
Hu, B., Ge, X., Wang, L.F., Shi, Z., 2015. Bat origin of human coronaviruses. Virol. J. 12, 221.
Inoue, Y., Tanaka, N., Tanaka, Y., Inoue, S., Morita, K., Zhuang, M., Hattori, T., Sugamura, K., 2007. Clathrin-dependent entry of severe acute respiratory syndrome coronavirus into target cells expressing ace2 with the cytoplasmic tail deleted. J. Virol. 81, 8722–8729.
Itoh, T., Takenawa, T., 2004. Regulation of endocytosis by phosphatidylinositol 4,5-bisphosphate and enth proteins. Curr. Top. Microbiol. Immunol. 282, 31–47.
Kaksonen, M., Roux, A., 2018. Mechanisms of clathrin-mediated endocytosis. Nat. Rev. Mol. Cell Biol. 19, 313–326.
Karthika, T., Joseph, J., Das, V.R.A., Nair, N., Charulekha, P., Roji, M.D., Raj, V.S., 2021. Sars-cov-2 cellular entry is independent of the ace2 cytoplasmic domain signaling. Cells 10, 1814.
Koch, J., Uckeley, Z.M., Doldan, P., Stanifer, M., Boulant, S., Lozach, P.Y., 2021. Tmprss2 expression dictates the entry route used by sars-cov-2 to infect host cells. EMBO J. 40, e107821.
Kumari, S., Mg, S., Mayor, S., 2010. Endocytosis unplugged: multiple ways to enter the cell. Cell Res. 20, 256–275.
Lambert, D.W., 2009. The Cell Biology of the Sars Coronavirus Receptor, Angiotensin-Converting Enzyme 2. Molecular Biology of the SARS-Coronavirus (chapter 2).
Lan, J., Ge, J., Yu, J., Shan, S., Zhou, H., Fan, S., Zhang, Q., Shi, X., Wang, Q., Zhang, L., Wang, X., 2020. Structure of the sars-cov-2 spike receptor-binding domain bound to the ace2 receptor. Nature 581, 215–220.
Li, W., Moore, M.J., Vasilieva, N., Sui, J., Wong, S.K., Berne, M.A., Somasundaran, M., Sullivan, J.L., Luzuriaga, K., Greenough, T.C., Choe, H., Farzan, M., 2003. Angiotensin-converting enzyme 2 is a functional receptor for the sars coronavirus. Nature 426, 450–454.
Li, G., Su, B., Fu, P., Bai, Y., Ding, G., Li, D., Wang, J., Yang, G., Chu, B., 2021a. Npc1-regulated dynamic of clathrin-coated pits is essential for viral entry. Sci. China Life Sci. 65, 341–361.
Li, X., Zhu, W., Fan, M., Zhang, J., Peng, Y., Huang, F., Wang, N., He, L., Zhang, L., Holmdahl, R., Meng, L., Lu, S., 2021b. Dependence of sars-cov-2 infection on

cholesterol-rich lipid raft and endosomal acidification. Comput. Struct. Biotechnol. J. 19, 1933–1943.
Lu, J.C., Chiang, Y.T., Lin, Y.C., Chang, Y.T., Lu, C.Y., Chen, T.Y., Yeh, C.S., 2016. Disruption of lipid raft function increases expression and secretion of monocyte chemoattractant protein-1 in 3t3-l1 adipocytes. PLoS One 11, e0169005.
Marks, M.S., Ohno, H., Kirchnausen, T., Bonracino, J.S., 1997. Protein sorting by tyrosine-based signals: adapting to the ys and wherefores. Trends Cell Biol. 7, 124–128.
McMahon, H.T., Boucrot, E., 2011. Molecular mechanism and physiological functions of clathrin-mediated endocytosis. Nat. Rev. Mol. Cell Biol. 12, 517–533.
McPherson, P.S., Kay, B.K., Hussain, N.K., 2001. Signaling on the endocytic pathway. Traffic 2, 375–384.
Miettinen, H.M., Matter, K., Hunziker, W., Rose, J.K., Mellman, I., 1992. Fc receptor endocytosis is controlled by a cytoplasmic domain determinant that actively prevents coated pit localization. J. Cell Biol. 116, 875–888.
Mirre, C., Monlauzeur, L., Garcia, M., Delgrossi, M.H., Le Bivic, A., 1996. Detergent-resistant membrane microdomains from caco-2 cells do not contain caveolin. Am. J. Physiol. 271, C887–C894.
Mlcochova, P., Kemp, S.A., Dhar, M.S., Papa, G., Meng, B., Ferreira, I., Datir, R., Collier, D.A., Albecka, A., Singh, S., Pandey, R., Brown, J., Zhou, J., Goonawardane, N., Mishra, S., Whittaker, C., Mellan, T., Marwal, R., Datta, M., Sengupta, S., Ponnusamy, K., Radhakrishnan, V.S., Abdullahi, A., Charles, O., Chattopadhyay, P., Devi, P., Caputo, D., Peacock, T., Wattal, C., Goel, N., Satwik, A., Vaishya, R., Agarwal, M., Indian, S.-C.-G.C., , Genotype to Phenotype Japan C, Collaboration, C.-N.B.C.-, Mavousian, A., Lee, J.H., Bassi, J., Silacci-Fegni, C., Saliba, C., Pinto, D., Irie, T., Yoshida, I., Hamilton, W.L., Sato, K., Bhatt, S., Flaxman, S., James, L.C., Corti, D., Piccoli, L., Barclay, W.S., Rakshit, P., Agrawal, A., Gupta, R.K., 2021. Sars-cov-2 b.1.617.2 delta variant replication and immune evasion. Nature 599, 114–119.
Montesano, R., Roth, J., Robert, A., Orci, L., 1982. Non-coated membrane invaginations are involved in binding and internalization of cholera and tetanus toxins. Nature 296, 651–653.
Morse, E.M., Brahme, N.N., Calderwood, D.A., 2014. Integrin cytoplasmic tail interactions. Biochemistry 53, 810–820.
Ng Sht, M.L., See, E.E., Ooi, E.E., Ling, A.E., 2003. Early events of sars coronavirus infection in vero cells. J. Med. Virol. 71, 323–331.
Orlandi, P.A., Fishman, P.H., 1998. Filipin-dependent inhibition of cholera toxin: evidence for toxin internalization and activation through caveolae-like domains. J. Cell Biol. 141, 905–915.
Ou, X., Liu, Y., Lei, X., Li, P., Mi, D., Ren, L., Guo, L., Guo, R., Chen, T., Hu, J., Xiang, Z., Mu, Z., Chen, X., Chen, J., Hu, K., Jin, Q., Wang, J., Qian, Z., 2020. Characterization of spike glycoprotein of sars-cov-2 on virus entry and its immune cross-reactivity with sars-cov. Nat. Commun. 11, 1620.
Planas, D., Veyer, D., Baidaliuk, A., Staropoli, I., Guivel-Benhassine, F., Rajah, M.M., Planchais, C., Porrot, F., Robillard, N., Puech, J., Prot, M., Gallais, F., Gantner, P., Velay, A., Le Guen, J., Kassis-Chikhani, N., Edriss, D., Belec, L., Seve, A., Courtellemont, L., Pere, H., Hocqueloux, L., Fafi-Kremer, S., Prazuck, T., Mouquet, H., Bruel, T., Simon-Loriere, E., Rey, F.A., Schwartz, O., 2021. Reduced sensitivity of sars-cov-2 variant delta to antibody neutralization. Nature 596, 276–280.
Posor, Y., Eichhorn-Grunig, M., Haucke, V., 2015. Phosphoinositides in endocytosis. Biochim. Biophys. Acta 1851, 794–804.
Rahman, F.I., Ether, S.A., Islam, M.R., 2021. The "delta plus" covid-19 variant has evolved to become the next potential variant of concern: mutation history and measures of prevention. J. Basic Clin. Physiol. Pharmacol. 33, 109–112.
Sanders, D.W., Jumper, C.C., Ackerman, P.J., Bracha, D., Donlic, A., Kim, H., Kenney, D., Castello-Serrano, I., Suzuki, S., Tamura, T., Tavares, A.H., Saeed, M., Holehouse, A.S., Ploss, A., Levental, I., Douam, F., Padera, R.F., Levy, B.D., Brangwynne, C.P., 2021. Sars-cov-2 requires cholesterol for viral entry and pathological syncytia formation. Elife 10, e65962.
Sorkin, A., von Zastrow, M., 2009. Endocytosis and signalling: intertwining molecular networks. Nat. Rev. Mol. Cell Biol. 10, 609–622.
Stan, R.V., 2005. Structure of caveolae. Biochim. Biophys. Acta 1746, 334–348.
Tang, T., Bidon, M., Jaimes, J.A., Whittaker, G.R., Daniel, S., 2020. Coronavirus membrane fusion mechanism offers a potential target for antiviral development. Antivir. Res. 178, 104792.
Tipnis, S.R., Hooper, N.M., Hyde, R., Karran, E., Christie, G., Turner, A.J., 2000. A human homolog of angiotensin-converting enzyme. Cloning and functional expression as a captopril-insensitive carboxypeptidase. J. Biol. Chem. 275, 33238–33243.
Towler, P., Staker, B., Prasad, S.G., Menon, S., Tang, J., Parsons, T., Ryan, D., Fisher, M., Williams, D., Dales, N.A., Patane, M.A., Pantoliano, M.W., 2004. Ace2 x-ray structures reveal a large hinge-bending motion important for inhibitor binding and catalysis. J. Biol. Chem. 279, 17996–18007.
Tran, D., Carpentier, J.L., Sawano, F., Gorden, P., Orci, L., 1987. Ligands internalized through coated or noncoated invaginations follow a common intracellular pathway. Proc. Natl. Acad. Sci. U. S. A. 84, 7957–7961.
Turner, A.J., Tipnis, S.R., Guy, J.L., Rice, G., Hooper, N.M., 2002. Aceh/ace2 is a novel mammalian metallocarboxypeptidase and a homologue of angiotensin-converting enzyme insensitive to ace inhibitors. Can. J. Physiol. Pharmacol. 80, 346–353.
von Kleist, L., Stahlschmidt, W., Bulut, H., Gromova, K., Puchkov, D., Robertson, M.J., MacGregor, K.A., Tomilin, N., Pechstein, A., Chau, N., Chircop, M., Sakoff, J., von Kries, J.P., Saenger, W., Krausslich, H.G., Shupliakov, O., Robinson, P.J., McCluskey, A., Haucke, V., 2011. Role of the clathrin terminal domain in regulating coated pit dynamics revealed by small molecule inhibition. Cell 146, 471–484.
Walls, A.C., Park, Y.J., Tortorici, M.A., Wall, A., McGuire, A.T., Veesler, D., 2020. Structure, function, and antigenicity of the sars-cov-2 spike glycoprotein. Cell 181, 281–292 e286.
Wang, H., Yang, P., Liu, K., Guo, F., Zhang, Y., Zhang, G., Jiang, C., 2008. Sars coronavirus entry into host cells through a novel clathrin- and caveolae-independent endocytic pathway. Cell Res. 18, 290–301.
White, J.M., Whittaker, G.R., 2016. Fusion of enveloped viruses in endosomes. Traffic 17, 593–614.
Who, 2021. Tracking Sars-Cov-2 Variants. WHO. https://www.who.int/en/activities/tracking-SARS-CoV-2-variants/. (Accessed 15 November 2021).
Wrapp, D., Wang, N., Corbett, K.S., Goldsmith, J.A., Hsieh, C.L., Abiona, O., Graham, B.S., McLellan, J.S., 2020. Cryo-em structure of the 2019-ncov spike in the prefusion conformation. Science 367, 1260–1263.
Yan, R., Zhang, Y., Li, Y., Xia, L., Guo, Y., Zhou, Q., 2020. Structural basis for the recognition of sars-cov-2 by full-length human ace2. Science 367, 1444–1448.
Yang, N., Ma, P., Lang, J., Zhang, Y., Deng, J., Ju, X., Zhang, G., Jiang, C., 2012. Phosphatidylinositol 4-kinase iiibeta is required for severe acute respiratory syndrome coronavirus spike-mediated cell entry. J. Biol. Chem. 287, 8457–8467.
Yang, H., Zhao, X., Xun, M., Ma, C., Wang, H., 2021. Reverse genetic approaches for the generation of full length and subgenomic replicon of ev71 virus. Front. Microbiol. 12, 665879.
Zoncu, R., Perera, R.M., Sebastian, R., Nakatsu, F., Chen, H., Balla, T., Ayala, G., Toomre, D., De Camilli, P.V., 2007. Loss of endocytic clathrin-coated pits upon acute depletion of phosphatidylinositol 4,5-bisphosphate. Proc. Natl. Acad. Sci. U. S. A. 104, 3793–3798.